Shen *et al.*
Chinese Journal of Mechanical Engineering (2024) 37:53
https://doi.org/10.1186/s10033-024-01032-6

ORIGINAL ARTICLE

Open Access

A Coordinate-Free Approach to the Design of Generalized Griffis-Duffy Platforms

Chengwei Shen[1,2], Xu Pei[2], Lubin Hang[3] and Jingjun Yu[2*]

Abstract

Architectural singularity belongs to the Type II singularity, in which a parallel manipulator (PM) gains one or more degrees of freedom and becomes uncontrollable. PMs remaining permanently in a singularity are beneficial for linear-to-rotary motion conversion. Griffis-Duffy (GD) platform is a mobile structure admitting a Bricard motion. In this paper, we present a coordinate-free approach to the design of generalized GD platforms, which consists in determining the shape and attachment of both the moving platform and the fixed base. The generalized GD platform is treated as a combination of six coaxial single-loop mechanisms under the same constraints. Owing to the inversion, hidden in the geometric structure of these single-loop mechanisms, the mapping from a line to a circle establishes the geometric transformation between the fixed base and the moving platform based on the center of inversion, and describes the shape and attachment of the generalized GD platform. Moreover, the center of inversion not only identifies the location of rotation axis, but also affects the shape of the platform mechanism. A graphical construction of generalized GD platforms using inversion, proposed in the paper, provides geometrically feasible solutions of the manipulator design for the requirement of the location of rotation axis.

Keywords Generalized Griffis-Duffy platforms, Self-motion, Inversion, Coordinate-free determination, Manipulator design

1 Introduction

When both the moving platform and the fixed base fulfill particular conditions, the Stewart-Gough (SG) platform can still admit a continuous motion, although all six linear actuators are locked at equal length, which is called self-motion. Indeed, the manipulator that undergoes the self-motion is singular in every possible configuration inside the whole workspace. These continuous singular configurations rather than discrete ones, merely caused by design parameters, were defined as architectural singularity. The notion was first introduced by Ma and Angeles in 1991 [1], and later widely used within the robotics community. On the one hand, architectural singularity belongs to the Type II singularity [2], in which a parallel manipulator (PM) gains one or more degrees of freedom and becomes uncontrollable. Thus, architectural singularity should be avoided for general applications. On the other hand, PMs remaining permanently in a singularity can be useful due to the capability of generating complex motions with only one actuator [3]. An energy regenerative suspension based on the architecturally singular platform was presented in Ref. [4], with the aim of converting vibratory linear motion into rotary motion.

Over the past decades, most investigations into architectural singularity concentrated on SG platforms [5], consisting in the characterization of self-motions and design conditions. Husty and Karger [6] made a classification of all self-motions of the original SG platform, which contains translations, rotations, generalized screw

*Correspondence:
Jingjun Yu
jjyu@buaa.edu.cn
[1] College of Optical, Mechanical and Electrical Engineering, Zhejiang A&F University, Hangzhou 311300, China
[2] School of Mechanical Engineering and Automation, Beihang University, Beijing 100191, China
[3] School of Mechanical and Automotive Engineering, Shanghai University of Engineering Science, Shanghai 201620, China

motions, and other complex spatial motions. Refs. [7, 8] gave the projective characterization of architecturally singular planar and non-planar SG platforms and indicated that they are invariant. Borras et al. [9, 10] provided a novel geometric interpretation for a class of architecturally singular line-plane 5-SPU platforms (S stands for a spherical joint, P stands for an prismatic joint, U stands for an universal joint), which in fact are the degenerated 6-SPS PMs. Nawratil [11] classified one-parametric self-motions of a general planar SG platform into two types. These publications followed a roadmap of analysis, synthesizing architecturally singular mechanisms may be an interesting topic. Kong [12] proposed a component method for the generation of singular SG platforms. Based on the location of limb attachments on the platforms, Wohlhart [13] constructed four types of mobile 6-SPS PMs with locked actuators. Lee and Herve [14] focused on the mechanical generation of the one degree of freedom Bricard motion and described a general structure with six SS kinematic chains, which can produce such motion. It should be emphasized that the manipulators possessing self-motions are not equivalent to architecturally singular manipulators. Ref. [15] presented a complete list of architecturally singular SG platforms with multidimensional self-motions. The phenomenon of self-motions also appears in a few other PMs. Briot et al. showed that the 3-RPR PM (R stands for a revolute joint) with similar platforms and zero offsets [16] and the Pantopteron robot [17] can admit the Cardanic self-motion. The movement also exists in the 3-PPPS PM [18]. Refs. [19, 20] discussed the self- motions of different types of 3-RPS PMs, which can be the butterfly motion and the spherical four-bar motion. From a theoretical point of view, the determination of these self-motions is closely related to the singularity analysis of the 6-3 type SG platform. Nurahmi et al. [21] detected the conditions for self-motions of a 4-CRU PM (C stands for a cylindrical joint). Wu and Bai [22] proposed an analytic approach to the determination of architectural singularity, the presence of self-motions were validated in the 3-PPR planar PM and the 3-PPS spatial PM.

The aim of this paper is to present a coordinate-free approach to the design of generalized Griffis-Duffy (GD) platforms, which consists in determining the shape and attachment of both the moving platform and the fixed base. The GD platform [23] is a special 6-6 type parallel manipulator with planar triangular platforms. Ref. [24] investigated the self-motions of a class of GD platforms and indicated that the manipulator can admit a one degree of freedom Bricard motion. We focus on the mechanical generation of such motion based on the geometric construction of generalized GD platforms. Our study cannot contribute to the design of any novel manipulators, but it provides an insight of synthesis for architecturally singular GD platforms. With the introduction of inversion, it will be shown that the mapping from a line to a circle reveals the geometric transformation between the moving platform and the fixed base of the GD platform. The center of inversion plays such an important role that affects the position of rotation axis. The approach, proposed in this paper, addresses the feasible solutions to the topology design of generalized GD platforms concerned with the location of rotation axis.

The rest of this paper includes five sections, which are organized as follows. Section 2 provides the concept of inversion and the subject of our investigation. Section 3 gives the relation between an inversion and a series of single-loop SSC mechanisms under the same algebraic constraints. Section 4 deals with the coordinate-free determination of a generalized GD platform using inversion. The effect of the center of inversion on the graphical construction is discussed in Section 5. Finally, Section 6 summarizes the main points of our study.

2 Preliminaries

2.1 Geometric Inversion

Inversion, a particular geometric transformation, will be applied as a powerful tool to the determination of the GD platform in our work. The concept of inversion is introduced as follows. More about the topic can be referred to Ref. [25]. Given an inversion $\boldsymbol{I}(O, \mu)$ and a point P other than the point O, the point Q on the ray OP is the inverse of the point P, if and only if:

$$|OP| \cdot |OQ| = \mu > 0. \tag{1}$$

It is noted that the symbol $|\bullet|$ denotes the Euclidean distance between two points in this paper. The relationship between the points P and Q, expressed as Eq. (1) is called an inversion, while point O is called the center of inversion, and constant μ is called the power of inversion.

The inversion indeed describes a constraint of a pair of points with respect to a fixed point, i.e., the center of inversion. These three points are collinear, and the product of the distance from one to the center with the distance from the other to the center is constant. Such a constraint is hidden in the geometric structure of the GD platform. It follows that generalized GD platforms can be characterized and synthesized by inversion, which will be discussed in this paper.

2.2 Generalized Griffis-Duffy Platforms

A midpoint-to-vertex Griffis-Duffy platform is presented schematically in Figure 1. The mobile structure consists of a fixed base and a moving platform connected to each other through six limbs, after locking all the extensible actuators of the SPS kinematic chains. Both the fixed base

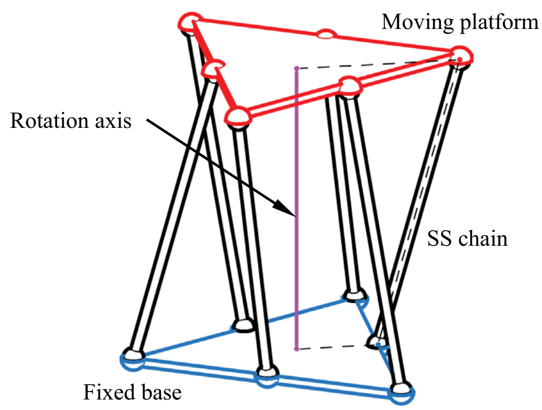

Figure 1 Midpoint-to-vertex Griffis-Duffy platform

and the moving platform are equilateral triangular plates. Each vertex of the fixed base is linked to the midpoint of the side of the moving platform, and each midpoint of the side of the fixed base is linked to the vertex of the moving platform. The moving platform can undergo a continuous Bricard motion [14, 24], which is a rotation about a certain axis, perpendicular to the fixed base, with parasitic translation along the axis, as depicted in Figure 1.

In this paper, we focus on the generalized GD platform, in which the shape and attachment of the fixed base and the moving platform is different from the midline-to-vertex GD platform, but the manipulator still admit a continuous Bricard motion.

3 Equivalent Mechanism with a Bricard Motion

Since there exists a virtual rotation axis in the GD platform, we start our study from the equivalent mechanism [5], which can admit a Bricard motion. A single-loop SSC mechanism appearing in Figure 2(a) is therefore taken into consideration. Let point P be the anchor point of the S joint attached to the fixed base, and point Q be the anchor point of the S joint attached to the moving platform. Point O is the foot of the perpendicular obtained from P to the axis of the C joint, and point O' is the foot of the perpendicular obtained from Q to the C joint axis. The dimension of the fixed base is defined as the distance from the anchor point P of the fixed S joint to the C joint axis, while the dimension of the moving platform is defined as the distance from the anchor point Q of the moving S joint to the C joint axis. For the equivalent mechanism, the moving platform $O'Q$ can translate along the C joint axis and rotate about the axis.

A reference frame $\{Oxyz\}$ is attached to the fixed base, in which the x-axis coincides with OP and the z-axis coincides with OO'. Therefore, the pose of the moving platform with respect to the fixed base is determined by the height s ($s \geq 0$), which is measured from O to O', and the angle θ ($\theta \geq 0$), which is measured from Ox to $O'Q$. Note that the kinematics of the mechanism has been studied in Refs. [14, 26]. Here, the constraint equation of the mechanism is given by:

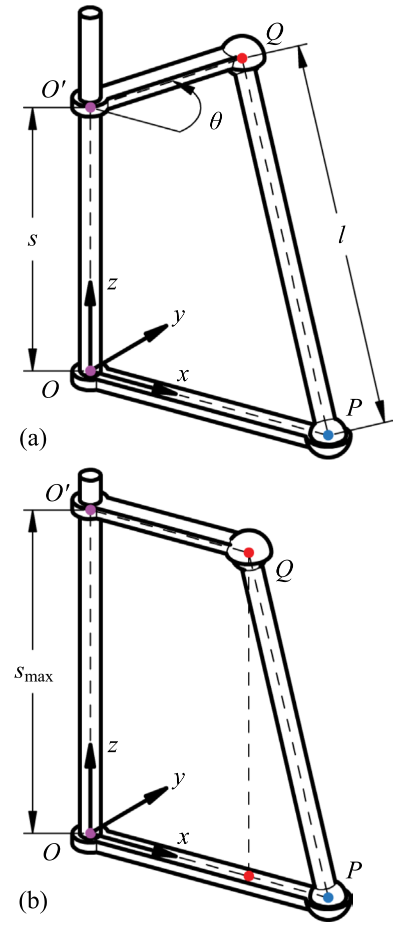

Figure 2 Schematic diagram of the equivalent mechanism

$$2 \cdot |OP| \cdot \left|O'Q\right| \cdot \cos\theta + |PQ|^2 - |OP|^2 - \left|O'Q\right|^2 = s^2. \tag{2}$$

As depicted in Figure 2(b), the moving platform is located at the home configuration of the single-loop SSC mechanism, in which the four points O, O', P and Q are coplanar.

Let θ be zero, then Eq. (2) is rewritten as:

$$2 \cdot |OP| \cdot \left|O'Q\right| + |PQ|^2 - |OP|^2 - \left|O'Q\right|^2 = s_{\max}^2, \tag{3}$$

where $s_{\max}$ denotes the maximal height, which the moving platform can reach. Taking the system of Eqs. (2) and (3) into consideration, we have:

$$2 \cdot |OP| \cdot \left|O'Q\right| \cdot (\cos\theta - 1) + s_{\max}^2 = s^2, \tag{4}$$

which indicates that the pose (s, θ) of the single-loop SSC mechanism is constrained by the dimensions of links,

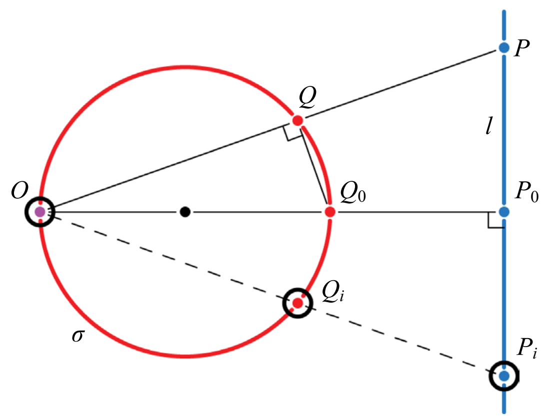

Figure 3 Transformation from a line to a circle

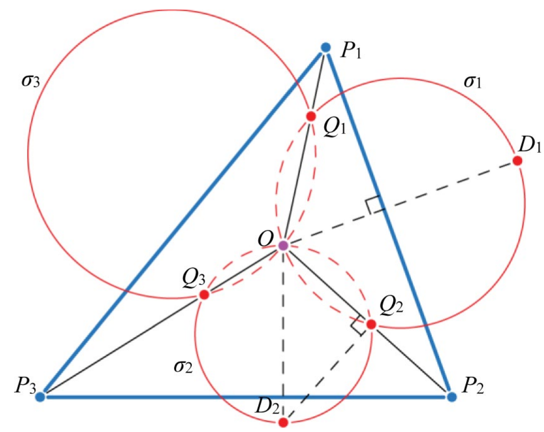

Figure 4 Circles are inverted from the sides of a given triangle

including the maximal height $s_{\max}$ of the moving platform located at the home configuration and the product of the dimension of the moving platform with the dimension of the fixed base. Let the product be:

$$\mu = |OP| \cdot |O'Q|, \tag{5}$$

then Eq. (4) can be reformulated as:

$$2 \cdot \mu \cdot (\cos\theta - 1) + s_{\max}^2 = s^2. \tag{6}$$

Eq. (6) constitutes the algebraic constraint for the single-loop SSC mechanism, any of these mechanism can be described by the formulation. Once the maximal height $s_{\max}$ is confirmed, the functional relation of two pose variables s and θ, expressed by Eq. (6), only depends on the unique factor μ. In this way, all the single-loop SSC mechanisms with the same constraints but different dimensions can be characterized by the factor μ. In other words, all the mechanisms with the same factor, which is the value of the product of the dimension of the moving platform with the dimension of the fixed base, can admit the same motion output.

The projection of the mechanism, when the moving platform is located at the home configuration, along the C joint axis onto the plane defined by the axes Ox and Oy is depicted in Figure 2(b). The point O determined by the location of the C joint, the anchor point P of the fixed S joint, and the projection of the point Q of the moving S joint are collinear. Then the factor μ in Eq. (5) can be rewritten as:

$$\mu = |OP| \cdot |OQ|, \tag{7}$$

which corresponds to Eq. (1). For a common assignment of the maximal height, a series of single-loop SSC mechanisms under the same constraints is characterized by the only factor μ, independent of the dimensions of links. Any of them can be described as three collinear points satisfying Eq. (7), while the point O stands for the location of the C joint, and a pair of inverse points P and Q with respect to the inversion $\boldsymbol{I}(O, \mu)$ represents the anchor points of the S joints.

Based on the projection of the single-loop SSC mechanism along the C joint axis, the description of a series of single-loop SSC mechanisms under the same constraints is linked to the concept of inversion. All of these mechanisms can admit the same motion output, although the dimensions of them are different. The link is free of dimensions and will be utilized for the graphical construction of generalized GD platforms.

4 Coordinate-Free Determination of Generalized GD Platforms

As a result of the existence of certain rotation axis, the self-motion of a generalized GD platform is equivalent to the motion output of a single-loop SSC mechanism. For a generalized GD platform, the moving platform is constrained by six SS limbs. Thus, the generalized GD platform can be regarded as a combination of six coaxial single-loop SSC mechanisms admitting the same Bricard motion. These mechanisms are under the same constraints and share the same factor μ, which has been analyzed in Section 3.

In this section, two key points to the determination of generalized GD platforms are addressed. The one is the construction of a series of coaxial single-loop SSC mechanisms under the same constraints. The other is the location of anchor points of S joints for the rational attachment of the fixed base and the moving platform, which will be performed by the arrangement of limbs from the view of vertical projection.

Go back to the concept of inversion, the mathematical notion not only describes a constraint of a pair of points with respect to a fixed point, but also establishes a geometric transformation on account of the fixed point, which maps a line to a circle under the constraint. The mapping under an inversion provides a graphical way directly for the construction of generalized GD platforms from an arbitrary triangle. A coordinate-free approach to the design of generalized GD platforms is presented thereupon.

4.1 Geometric Inversion

The inversion, in nature, maps one point to another on a ray from the center of the inversion. By taking the inverse of each point of a figure with respect to a center, the inverse of the figure can be obtained, which appears as a geometric transformation between the two figures. There are anchor points being located on the sides of platforms in the generalized GD platform, the inverse of points lying on a line is first taken into consideration.

As shown in Figure 3, let point P_0 be the foot of the perpendicular from point O to line l, and point Q_0 be the inverse of P_0 under the inversion $\boldsymbol{I}(O,\ \mu)$. Suppose that any point P on l other than P_0 has an inverse point Q with respect to the point O, then they obey:

$$|OP| \cdot |OQ| = |OP_0| \cdot |OQ_0| = \mu. \tag{8}$$

There exists an identity for triangles QOQ_0 and P_0OP as follows:

$$\angle QOQ_0 \equiv \angle P_0OP. \tag{9}$$

In accordance with the Side-Angle-Side similarity criterion, it can be concluded that:

$$\Delta QOQ_0 \sim \Delta P_0OP. \tag{10}$$

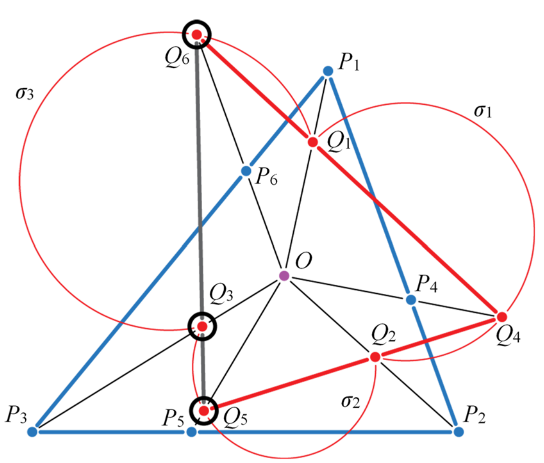

Figure 5 Moving platform generated from a fixed base

Thus, we have:

$$\angle Q_0QO = \angle PP_0O = \frac{\pi}{2}, \tag{11}$$

which implies that point Q lies on the circle σ with diameter OQ_0.

The above derivation indicates that a line l can be mapped to a circle σ under an inversion with the center O. The circle passes through the center of inversion and the tangent to the circle at the center is parallel to the line. As introduced in Section 2, an inversion is defined by a certain center and a constant power. However, it is concluded that a line can be inverted into a circle that passes through the center of inversion, while the power of inversion keeps unknown but constant. Thus, this geometric transformation from the line to the circle is independent of the power of inversion.

Thanks to the mapping based on the inversion, there is a one-to-one correspondence between points on l and points on σ. Consider a series of coaxial single-loop SSC mechanisms with the same constraints, all the mechanisms are characterized by the factor μ, which corresponds to the power of inversion. Any of them, denoted by subscript i, can be described by three collinear points O, P_i and Q_i. Among them, point O stands for the location of the C joint axis, points P_i represent the anchor points of the fixed S joints, and points Q_i represent the anchor points of the moving S joints. Then all the points Q_i, except for O, on the circle σ are the inverse points of P_i on the line l. Owing to the property of inversion, the points O, P_i and Q_i obey:

$$|OP_i| \cdot |OQ_i| = \text{constant}. \tag{12}$$

All the coaxial single-loop SSC mechanisms can realize the same motion output, in which anchor points of the fixed base lie on the line drawn in blue, and anchor points of the moving platform lie the circle drawn in red, as shown in Figure 3. Note that if the moving anchor point Q_i lies on l, its inverse, i.e., the fixed anchor point P_i lies on σ.

Contributed by the independence of the power of inversion in the geometric transformation from a line to a circle, a series of coaxial single-loop SSC mechanisms with the same motion output are constructed by a line and an inverted circle, based on a point defined as the center of inversion. The center indeed performs as the C joint axis of these coaxial mechanisms.

4.2 Construction of a Generalized GD Platform

Based on the mapping from a line to a circle, a series of coaxial single-loop SSC mechanisms with the same factor μ are constructed. The generalized GD platform will be

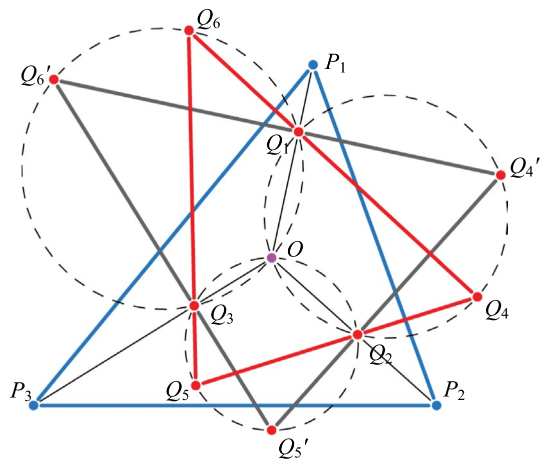

Figure 6 Two different triangles generated from a given triangle

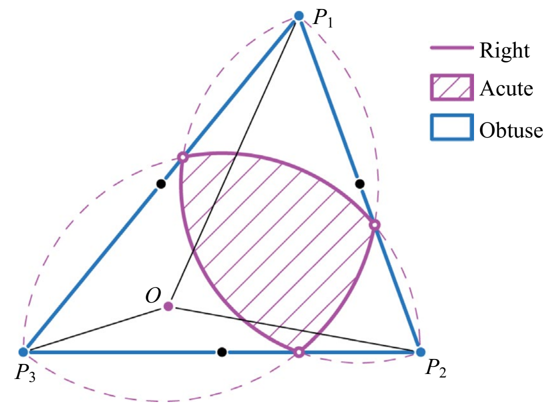

Figure 7 Different regions which can generate right, acute and obtuse triangles

generated from an arbitrary triangle by taking inverses of three sides respectively.

Denote P_i and Q_i as the anchor points of the S joints on the fixed base and the moving platform, respectively. Given an arbitrary triangle, defined by P_1, P_2 and P_3, as the fixed base, any point O inside it is selected as the center of inversion. As illustrated in Figure 4, the inverted circle σ_1 from side P_1P_2 is obtained by any diameter OD_1 perpendicular to P_1P_2. The circle σ_1 intersects the rays OP_1 and OP_2 at Q_1 and Q_2, respectively. Inverted from side P_2P_3, the second circle σ_2 through Q_2, with diameter OD_2 perpendicular to P_2P_3, intersects at the ray OP_3 at Q_3. Due to the power keeps constant, we have:

$$|OP_1| \cdot |OQ_1| = |OP_2| \cdot |OQ_2| = |OP_3| \cdot |OQ_3|, \quad (13)$$

which indicates that the circle σ_3 determined by the three points Q_1, O and Q_3 is the inverse of side P_1P_3. Because of the finite of segments, three sides are inverted respectively into three circular arcs under the inversion, as shown in Figure 4. For the sake of simplicity, both the circle and circular arc are denoted by σ_i.

According to the one-to-one correspondence between the points on the line and the points on the inverted circle, points P_i lying on the sides and Q_i lying on the inverted circular arcs, shown as Figure 5, satisfy:

$$|OP_i| \cdot |OQ_i| = |OP_1| \cdot |OQ_1| = |OP_2| \cdot |OQ_2| = |OP_3| \cdot |OQ_3|, \quad i = 4, 5, 6. \quad (14)$$

There exists a point, denoted by Q_4 , lying on the circle σ_1. Suppose that ray Q_4Q_2 intersects the circle σ_2 at Q_5 and ray Q_4Q_1 intersects the circle σ_3 at Q_6, as depicted in Figure 5. Considering that opposite angles are supplementary for the cyclic quadrilaterals $OQ_1Q_4Q_2$, $OQ_2Q_5Q_3$ and $OQ_3Q_6Q_1$, we have:

$$\begin{aligned} \angle OQ_1Q_4 + \angle OQ_2Q_4 &= \angle OQ_2Q_5 + \angle OQ_3Q_5 \\ &= \angle OQ_1Q_6 + \angle OQ_3Q_6 = \pi. \end{aligned} \quad (15)$$

Since points Q_4, Q_1 and Q_6 are collinear, so are points Q_4, Q_2 and Q_5, then we obtain:

$$\angle OQ_1Q_4 + \angle OQ_1Q_6 = \angle OQ_2Q_4 + \angle OQ_2Q_5 = \pi. \quad (16)$$

Thus, it can be concluded that:

$$\angle OQ_3Q_5 + \angle OQ_3Q_6 = \pi. \quad (17)$$

Finally, the shape of the moving platform and the arrangement of SS limbs, with respect to a triangle selected as the fixed base, has been determined graphically.

With the center of inversion O being selected inside the fixed base, a circle with arbitrary diameter through the point O is inverted from any one of three sides, then the other two inverted circles are obtained from the remaining sides, which determines the arrangement of three SS limbs connected between the vertex of the fixed base and the side of the moving platform. Two rays from a point lying on an inverted circular arcs constitute two sides of the moving platform. The existence of collinear points lying on the remaining two inverted circular arcs ensures the arrangement of the remaining three SS limbs connected between the side of the fixed base and the vertex of the moving platform. Finally, six coaxial single-loop SSC mechanisms are combined as a generalized GD platform, whose fixed base and moving platform are general

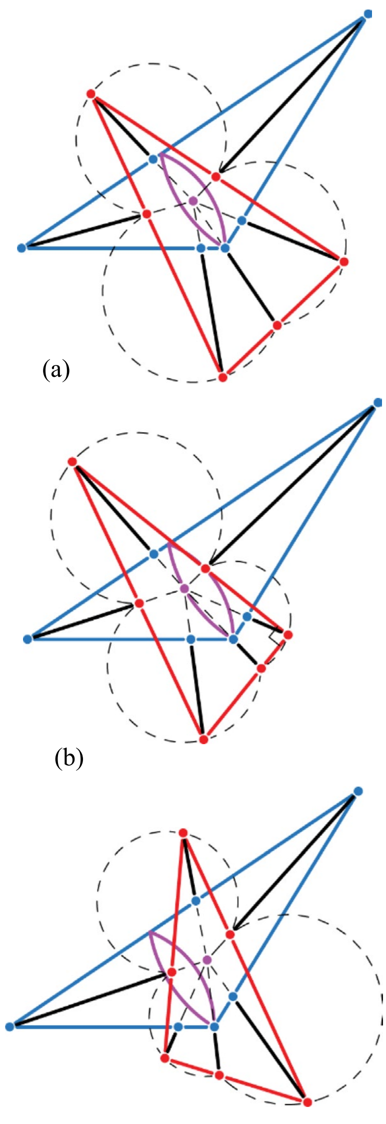

Figure 8 Moving platform generated from a fixed base

triangular plates. By the removal of the C joint shared by these mechanisms, the constructed manipulator can still realize a Bricard motion.

It should be noted that if a triangle is given as the moving platform, the other is then generated as the fixed base under the inversion, which can also achieve a generalized GD platform.

5 Discussion on the Construction

In the graphical construction of a generalized GD platform through the geometric transformation of inversion, which is free of the power of inversion, the center of inversion plays such a critical role that affects the shape of the generated triangle with respect to the given triangle.

Two different triangles are generated from a given $\Delta P_1P_2P_3$ based on three inverted circles, as depicted in Figure 6. The center of inversion O inside $\Delta P_1P_2P_3$ is selected, and three angles, P_1OP_2, P_2OP_3, and P_3OP_1, can be determined uniquely. It can be obtained that the four convex quadrilaterals $OQ_1Q_4Q_2$, $OQ_2Q_5Q_3$ and $OQ_3Q_6Q_1$ are cyclic, the opposite angles of each of them are supplementary, thus,

$$\begin{aligned}\angle Q_1OQ_2 + \angle Q_1Q_4Q_2 =& \angle Q_2OQ_3 + \angle Q_2Q_5Q_3 \\ =& \angle Q_1OQ_3 + \angle Q_1Q_6Q_3 = \pi.\end{aligned} \tag{18}$$

Since points O, P_i and Q_i are collinear, we get the following identities:

$$\begin{aligned}&\angle Q_6Q_4Q_5 = \pi - \angle P_1OP_2,\ \angle Q_4Q_5Q_6 = \pi - \angle P_2OP_3 \\ &\text{and } \angle Q_4Q_6Q_5 = \pi - \angle P_1OP_3.\end{aligned} \tag{19}$$

which indicates that the shape of the generated triangles is affected by the location of the center of inversion. For any point O inside $\Delta P_1P_2P_3$, we can obtain:

$$\begin{aligned}&\min\{\angle P_1OP_2, \angle P_2OP_3, \angle P_3OP_1\} > \\ &\min\{\angle P_1P_3P_2, \angle P_2P_1P_3, \angle P_3P_2P_1\}.\end{aligned} \tag{20}$$

In accordance with the supplementation of opposite angles in cyclic quadrilateral, the generated $\Delta Q_4Q_5Q_6$ obeys:

$$\begin{aligned}&\max\{\angle Q_6Q_4Q_5, \angle Q_4Q_5Q_6, \angle Q_4Q_6Q_5\} \\ &\quad = \pi - \min\{\angle P_1OP_2, \angle P_2OP_3, \angle P_1OP_3\}.\end{aligned} \tag{21}$$

Thus, we have:

$$\begin{aligned}&\max\{\angle Q_6Q_4Q_5, \angle Q_4Q_5Q_6, \angle Q_4Q_6Q_5\}+ \\ &\min\{\angle P_1P_3P_2, \angle P_2P_1P_3, \angle P_3P_2P_1\} < \pi.\end{aligned} \tag{22}$$

From Eq. (22), it shows that the shape of the generated moving platform, $\Delta Q_4Q_5Q_6$, is constrained by the shape of the given fixed base, $\Delta P_1P_2P_3$, besides the effect of the location of the center of inversion. In other word, it can be concluded that not any two triangles can be constructed as a generalized GD platform. Furthermore, Eq. (22) indicates the identification condition of a pair of triangles for the construction of generalized GD platforms.

Finally, the regions of locations of the center of inversion that lead to different shapes of generated triangles are depicted in Figure 7. The boundary between the regions that generate acute and obtuse triangles is identified by three circles with diameters obtained by

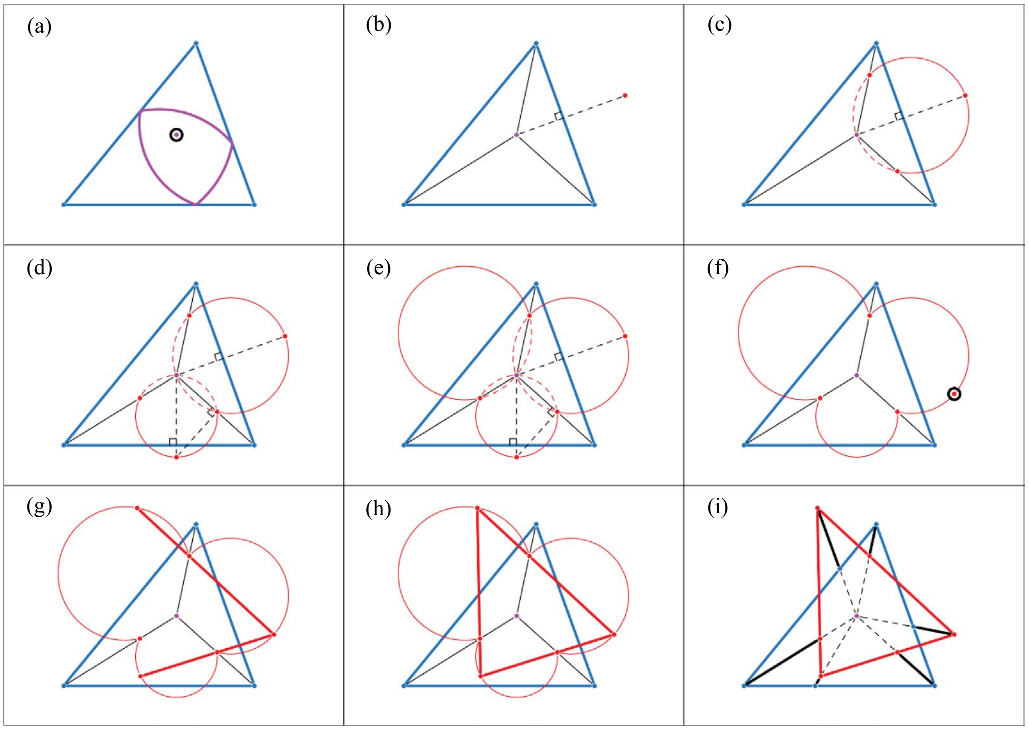

Figure 9 Schematic procedure for constructing a generalized GD platform with respect to the location of rotation axis

the sides of the given triangle, which can generate right triangles.

Taking an obtuse triangle given as the fixed base for instance, we generate the acute, right and obtuse triangles respectively, as depicted in Figure 8. Recall that if one triangle is given as the moving platform, the other is then generated as the fixed base under the inversion.

As mentioned before, the center of inversion stands for the C joint axis, which indeed indicates the location of the Bricard motion of the manipulator in the view of vertical projection. For the topology design of generalized GD platforms, we can obtain the geometrically feasible solutions, including the sharp and attachment of the fixed base and the moving platform, to meet the requirement of the location of rotation axis of the moving platform with respect to the fixed base through the map depicted as Figure 7. In addition, a schematic procedure for constructing a generalized GD platform with respect to the location of rotation axis, which contains nine steps from (a) to (i), is presented in Figure 9.

6 Conclusions

(1) This paper presents a coordinate-free approach to the design of generalized GD platforms. The generalized GD platform is regarded as a combination of six coaxial single-loop SSC mechanisms with different dimensions. These mechanisms are under the same constraints and admit the same Bricard motion, which are linked to the concept of inversion.

(2) Any of these mechanisms can be described by three collinear points, one stands for the location of the C joint axis, the remaining two represent the anchor points of the fixed base and the moving platform. Based on an arbitrary triangle as the fixed base, the shape of the moving platform and the arrangement of SS limbs are determined through the geometric transformation from a line to circle.

(3) On the one hand, the inversion from a line to a circle free of the power, provides a geometric approach for the non-dimensional construction of generalized GD platforms in the plane. The mapping from a line to a circle under the inversion performs as a geometric transformation and describes the shape and attachment of the fixed base and the moving platform of the generalized GD platform.

(4) On the other hand, the center of inversion plays a critical role in the generation. The point not only identifies the location of rotation axis of the generalized GD platform, but also affects the shape of the generated platform with respect to the given one. Thus, the proposed construction is a synthesis

of the generalized GD platform with the aim of the location rotation axis.

(5) An interesting conclusion, according to our investigation, is drawn that not any two triangles can be constructed as a generalized GD platform.

Acknowledgements
Not applicable.

Authors' Contributions
JY was in charge of the whole trial; CS wrote the manuscript; XP and LH assisted with drawing and spelling. All authors read and approved the final manuscript.

Funding
Supported by National Natural Science Foundation of China (Grant Nos. U1813221, 52075015), and Personnel Startup Project of Zhejiang A&F University Scientific Research Development Foundation of China (Grant No. 2024LFR015).

Data Availability
This paper investigated the design of general Griffis-Duffy platform, which is concerned with geometric construction, the result or conclusion is presented via graphics drawing. No data available.

Declarations

Competing Interests
The authors declare no competing financial interests.

Received: 13 July 2022 Revised: 8 April 2024 Accepted: 11 April 2024
Published online: 31 May 2024

References

[1] O Ma, J Angeles. Architecture singularities of platform manipulators. In: *Proceedings of the IEEE International Conference on Robotics and Automation*, Sacramento, April 9-11, 1991: 1542-1547.
[2] C Gosselin, J Angeles. Singularity analysis of closed-loop kinematic chains. *IEEE Transactions on Robotics and Automation*, 1990, 6(3): 281-290.
[3] J P Merlet, C Gosselin, T Huang. Parallel mechanisms. In: *Springer Handbook of Robotics*. Cham: Springer, 2016: 443-462.
[4] R Sabzehgar, A Maravandi, M Moallem. Energy regenerative suspension using an algebraic screw linkage mechanism. *IEEE/ASME Transactions on Mechatronics*, 2013, 19(4): 1251-1259.
[5] D Hartmann. *Singular Stewart-Gough platforms*. Montreal: McGill University, 1995.
[6] A Karger, M Husty. Classification of all self-motions of the original Stewart-Gough platform. *Computer-Aided Design*, 1998, 30(3): 205 -215.
[7] A Karger. Architecture singular planar parallel manipulators. *Mechanism and Machine Theory*, 2003, 38(11): 1149-1164.
[8] A Karger. Architecturally singular non-planar parallel manipulators. *Mechanism and Machine Theory*, 2008, 43(3): 335-346.
[9] J Borras, F Thomas, C Torras. Architectural singularities of a class of pentapods. *Mechanism and Machine Theory*, 2011, 46(8): 1107- 1120.
[10] J Borras, F Thomas, C Torras. Singularity-invariant families of line- plane 5-SPU platforms. *IEEE Transactions on Robotics*, 2011, 27(5): 837-848.
[11] G Nawratil. Types of self-motions of planar Stewart Gough platforms. *Meccanica*, 2013, 48(5): 1177-1190.
[12] X Kong. Generation of singular 6-SPS parallel manipulators. In: *International Design Engineering Technical Conferences and Computers and Information in Engineering Conference*, Atlanta, September 13-16, 1998: V01AT01A018.
[13] K Wohlhart. Mobile 6-SPS parallel manipulators. *Journal of Robotic Systems*, 2003, 20(8): 509-516.
[14] C C Lee, J M Herve. Bricard one-DoF motion and its mechanical generation. *Mechanism and Machine Theory*, 2014, 77: 35-49.
[15] G Nawratil. On Stewart Gough manipulators with multidimensional self-motions. *Computer Aided Geometric Design*, 2014, 31(7-8): 582-594.
[16] S Briot, V Arakelian, I A Bonev, et al. Self-motions of general 3-RPR planar parallel robots. *The International Journal of Robotics Research*, 2008, 27(7): 855-866.
[17] S B Briot, I A Bonev. Self motions of the pantopteron. In: *International Design Engineering Technical Conferences and Computers and Information in Engineering Conference*, San Diego, August 30-September 2, 2009: 633-638.
[18] D Chablat, E Ottaviano, S Venkateswaran. Self-motion conditions for a 3-PPPS parallel robot with delta-shaped base. *Mechanism and Machine Theory*, 2019, 135: 109-114.
[19] G Nawratil. Self-motions of TSSM manipulators with two parallel rotary axes. *ASME Journal of Mechanisms and Robotics*, 2011, 3(3): 031007.
[20] J Schadlbauer, M L Husty, S Caro, et al. Self-motions of 3-RPS manipulators. *Frontiers of Mechanical Engineering*, 2013, 8(1): 62-69.
[21] L Nurahmi, P Putrayudanto, G Wei, et al. Geometric constraint-based reconfiguration and self-motions of a four-CRU parallel mechanism. *ASME Journal of Mechanisms and Robotics*, 2021, 13(2): 021017.
[22] X Wu, S Bai. Analytical determination of shape singularities for three types of parallel manipulators. *Mechanism and Machine Theory*, 2020, 149: 103812.
[23] M W Griffis, J Duffy. Method and apparatus for controlling geometrically simple parallel mechanisms with distinctive connections. U.S. Patent No. 5179525. Washington, DC: U.S. Patent and Trademark Office, 1993.
[24] M Husty, A Karger. Self-motions of Griffis-Duffy type parallel manipulators. In: *Proceedings of the IEEE International Conference on Robotics and Automation*, San Francisco, April 24-28, 2000: 7-12.
[25] H Courant, R Courant, H Robbins, et al. *What is Mathematics?: An elementary approach to ideas and methods*. Oxford University Press, 1996.
[26] C Shen, L Hang. Synthesis of a type of self-motion mechanisms and the dimensional characteristic of ratio based on the construction of cognates. *Journal of Mechanical Engineering*, 2018, 54(19): 41-48. (in Chinese)

Chengwei Shen Born in 1992, is currently a lecturer at *College of Optical, Mechanical and Electrical Engineering, Zhejiang A&F University, China*. He received the Ph.D. degree from *Beihang University, China,* in June, 2023. His research interests include mechanisms and robotics.

Xu Pei Born in 1979, is currently an associate professor at *School of Mechanical Engineering and Automation, Beihang University, China*. His research interests include mechanisms and robotics.

Lubin Hang Born in 1965, is currently a professor at *School of Mechanical and Automotive Engineering, Shanghai University of Engineering Science, China*. His research interests include mechanisms and robotics.

Jingjun Yu Born in 1974, is currently a professor at *School of Mechanical Engineering &Automation, Beihang University, China*. His research interests include mechanisms and robotics.